Biochemical and Biophysical Research Communications 427 (2012) 587–592

Contents lists available at SciVerse ScienceDirect

Biochemical and Biophysical Research Communications

journal homepage: www.elsevier.com/locate/ybbrc

The functional role of UBA1 cysteine-278 in ubiquitination

Ung Yang [a,1], Hee-Young Yang [a,1], Jeong-Sun Kim [b], Tae-Hoon Lee [a,*]

[a] Department of Oral Biochemistry, Dental Science Research Institute and the BK21 Project, Medical Research Center for Biomineralization Disorders, School of Dentistry, Chonnam National University, Gwangju, Republic of Korea
[b] Department of Chemistry and Institute of Basic Sciences, Chonnam National University, Gwangju, Republic of Korea

ARTICLE INFO

Article history:
Received 17 September 2012
Available online 26 September 2012

Keywords:
Ubiquitin activating enzyme E1
Hyperoxidized cysteines
UBA1 activity
Ubiquitination

ABSTRACT

Although total UBA1 levels were unchanged, after oxidation for 60 min, we observed dramatic changes in the levels of BIAM-labeled UBA1 in both the membrane and cytosol fractions that suggested oxidative stress induces translocation of UBA1 from the cytosol to the membrane. Notably, in PrdxII$^{-/-}$ oxRBCs, ubiquitination levels were reduced about 75% in the membrane fraction after 90 min, even though UBA1 levels were increased. These results suggest ubiquitination levels are determined by UBA1 activity, not the level of UBA1 protein. Levels of ubiquitin conjugate (denoted ~Ub) in HEK293T and CMT93 cells transfected with UBA1(C278S) or UBA1(C632S) were lower than in cells expressing UBA1(WT) or another cysteine mutant. During the reaction, UBA1(WT)~Ub was nearly completely eliminated within 30 min, whereas UBA1(C278S)~Ub and UBA1(C632S)~Ub persisted. Within UBA1(C278S)~Ub, the catalytic cysteine (Cys-632) remained intact; nonetheless, migration of UBA1(C278S)~Ub and UBA1(C632S)~Ub were similar. These data suggest that Cys-278 can affect Ub charging through a change in the structural conformation of UBA1, not through direct interaction at the UBA1–Ub interface.

1. Introduction

Selective and regulated protein degradation via the ubiquitin–proteasome system is essential for maintenance of cellular homeostasis [1]. The ubiquitination process requires the coordinated action of three enzymes: ubiquitin (Ub)-activating enzyme (E1), Ub-conjugating enzyme (E2) and Ub ligase (E3) [2]. Ub is a highly conserved, 76-amino acid polypeptide that contains 7 lysine residues and a C-terminal di-glycine motif. The major function of Ub activating enzyme E1 (UBA1) is to promote degradation of damaged proteins by 26S proteasome by tagging the target proteins with an Ub moiety. UBA1 has two consensus sequences [3] that are highly conserved among human, mouse, rat, yeast and wheat (Fig. S1). UBA1 Cys-632 has been identified as a catalytic cysteine in an *in vitro* mutagenic study of conserved cysteines and a mass spectrometry study. Hatfield et al. showed that Cys-626 (Cys-632 in the mouse analog, Fig. S1) in wheat UBA1 is essential for forming a thioester bond with Ub [4]. In addition, Forrester et al. used the acyl-RAC technique to confirm that the *S*-acylation type catalyzed by UBA1 is glycyl-ubiquitin at Cys-632 [5].

In an earlier study, we detected hyperoxidized cysteines in some candidates in RBCs from PrdxII$^{-/-}$ mice [6]. It has been suggested that PrdxII acts as a redox regulator in RBCs, but it is unclear whether the accumulation of damaged proteins is caused by impaired ubiquitination. UBA1 contains four hyperoxidized cysteines (at positions 23, 278, 340 and 494 in mice) among its numerous cysteines (Fig. S1). Moreover, amino acid sequence alignment of UBA1 orthologs showed that these four hyperoxidized cysteine residues are conserved (Fig. S1), though their function remains unknown.

We hypothesized that oxidative stress-induced impairment of UBA1 activity may trigger the accumulation of protein aggregates due to the impaired ubiquitination. To test this hypothesis, we analyzed the ubiquitination pattern, UBA1 level, and UBA1 redox status in oxidized RBCs (oxRBCs) and designed five mutants (C23S, C278S, C340S, C494S and C632S). We also evaluated the relation between UBA1 activity and ubiquitination and the functional role of UBA1 Cys-278 in both *in vivo* and *in vitro* ubiquitination.

2. Materials and methods

2.1. Plasmids

To obtain a UBA1 mammalian expression vector, UBA1-Flag was amplified using primers 5′-CCGGGAATTCATGTCCAGCTCGCCGCTG-3′ and 5′-CCGGTCTAGATCACTTATCGTCGTCATCCTTGTAATCGCGG

Abbreviations: E1, ubiquitin activating enzyme; E2, ubiquitin conjugating enzyme; E3, ubiquitin ligase; FCCH, first catalytic cysteine half-domain; SCCH, second catalytic cysteine half-domain; Ub, ubiquitin; PrdxII, peroxiredoxin II; RBCs, red blood cells; oxRBCs, oxidized RBCs; PD, Parkinson's disease; AD, Alzheimer's disease.

* Corresponding author. Address: Department of Biochemistry, School of Dentistry, Chonnam National University, 300 Yongbong Dong, Buk-Ku, Gwangju 500-757, Republic of Korea. Fax: +82 62 5304848.
E-mail address: thlee83@chonnam.ac.kr (T.-H. Lee).
[1] These authors contributed equally to this work.

0006-291X/$ - see front matter © 2012 Elsevier Inc. All rights reserved.
http://dx.doi.org/10.1016/j.bbrc.2012.09.102

CCGCCGCGAATGGTATATCGGAC-3′ and subcloned into the *Eco*RI and *XbaI* sites of pCR3.1 (Invitrogen, USA) using UBA1 cDNA kindly provided by Dr. Seino (National Institute of Genetics, Japan). Cysteine residues in UBA1-Flag were replaced with serine at Cys-23 (C23S), Cys-278 (C278S), Cys-340 (C340S), Cys-494 (C494S) and Cys-632 (C632S) using the protocol provided with the GENEART® site-directed mutagenesis system (Invitrogen, USA). To generate a UBA1 *Escherichia coli* expression vector, His-tagged UBA1 WT, C278S or C632S was amplified using primers 5′-CCGGGAATTCATGTCCAGCTCGCCGCTG-3′ and 5′-CCGGCTCGAGTCAGCGAATGGTATATCG-3′, and then subcloned into the *Eco*RI and *XhoI* sites of pCR3.1. These constructs were then digested with *Eco*RI, *XbaI* and subcloned into pCold™ I (Takara, Japan). His-E2A was amplified using primers 5′-GGCCGGATCCATGTCGACCCCGGCCCGGCG-3′ and 5′-GGCCCTGCAGTCAACAGTCGCGCCAGCTTTG-3′, and subcloned into the *BamHI* and *PstI* sites of pRSET A (Invitrogen, USA) using a mMU004221 cDNA clone, which was a gift from the 21C Human Gene Bank, Genome Research Center, KRIBB, Korea. A His-tagged ubiquitin expression plasmid was a kind gift from Dr. H.Z. Chae (Chonnam National University, Korea).

2.2. Preparation of RBCs

OxRBCs (4% hematocrit in PBS) were prepared by incubating RBCs with 0.2 mM $CuSO_4$ and 5 mM ascorbic acid at 37 °C for the indicated times (0, 30, 60 or 90 min) [6]. BIAM labeling was performed as described previously [6]. After the incubation with BIAM, membrane and cytosolic proteins (250 μg and 2 mg, respectively) were incubated overnight with streptavidin-conjugated Sepharose beads (GE Healthcare, Sweden) at 4 °C on a shaker. The beads were then washed with IP buffer three times and boiled at 95 °C for 10 min. The IP proteins were then subjected to 12% SDS–PAGE, and western blotting was performed using primary antibodies against UBA1 (1:1000, CST, USA) and PrdxII (1:2000, Ab-Frontier), which were followed by HRP-conjugated secondary antibody (CST, USA).

2.3. Cell cultures and transfections

HEK293T and CMT93 cells were cultured in Dulbecco's modified Eagle's medium (GenDEPOT, USA) supplemented with 10% FBS (Gibco, USA) and 1% Pen/Strep (Invitrogen, USA). Twenty-four hours before transfection, cells were seeded at 40–60% confluency into 60-mm dishes. The cells were then co-transfected with 1 μg each of His-ubiquitin and either UBA1-Flag (wild-type) or a UBA1-Flag cysteine mutant (C23S, C278S, C340S, C494S or C632S) using Lipofectamine 2000 (Invitrogen, USA) according to the manufacturer's instructions. After 14 h, cells were pretreated with 10 μM MG132 (Merck, USA), and 0.1 mM cycloheximide (Sigma, USA) was added for the next 13 h. At 28 h after transfection, 0.2 mM H_2O_2 was added for 6 h. After the H_2O_2 treatment, the cells were lysed and sonicated in urea buffer (10 mM Tris–HCl, pH 7.5, 7 M urea, 2 M thiourea, 0.49% (w/v) CHAPS) supplemented with 1 mM DTT, a protease inhibitor cocktail (1 mM PMSF, 1 mM AEBSF, 1 μg/mL leupeptin, 1 μg/mL aprotinin, 1 μg/mL pepstatin) and a deubiquitinase inhibitor (10 mM IAA). Cell lysates were cleared by centrifugation at 13,000×*g* for 30 min at 4 °C, and proteins were quantified using BCA assays (Pierce, USA). Equal amounts of protein (30 μg/lane) were then separated by SDS–PAGE and immunoblotted with anti-Flag (1:1000, CST, USA), anti-His (1:1000, CST, USA) and anti-β-actin (1:5000, CST, USA) antibodies.

2.4. Recombinant protein expression and E1 enzymatic assay

His-tagged proteins were overexpressed in *E. coli* BL21(DE3)-pLysS and purified on Ni-affinity resins according to the manufacturer's instructions (Elpisbiotech, Korea). To assess UBA1 (wild-type, C278S, C632S) enzymatic activity *in vitro*, N-terminal His-tagged UBA1 (0.5 μM) and Flag-tagged ubiquitin (1 μM) were incubated in 10 μL of reaction buffer containing 50 mM Tris–HCl, pH 7.0, 5 mM $MgCl_2$, 1 mM DTT, 100 mM NaCl and 5 mM ATP for 30 min at 37 °C. The products were resolved on 10% SDS–PAGE under nonreducing conditions, after which the formation of UBA1∼Ub conjugates was assessed by immunoblotting. To determine the ubiquitin transfer to E2A, His-tagged UBA1 (0.5 μM), His-tagged E2A (1 μM) and Flag-tagged ubiquitin (1 μM) were incubated in 10 μL of reaction buffer containing 50 mM Tris–HCl, pH 7.0, 5 mM $MgCl_2$ and 1 mM ATP for 30 min at 37 °C. The products were resolved on nonreducing 10% SDS–PAGE followed by immunoblotting with anti-His antibody. Formation of E2A–Ub conjugates was detected using ECL reagent (iNtRON, Korea).

3. Results and discussion

3.1. Determination of the ubiquitination levels and UBA1 activity

In PrdxII$^{-/-}$ RBCs, ROS levels are elevated, and various abnormalities and aggregate formation have been reported [7]. Thus oxRBCs are now a well-established *in vitro* RBC oxidation model induced using $CuSO_4$ and ascorbic acid [8–10]. Intracellular aggregates of denatured hemoglobin are formed in oxRBCs, and it is these aggregates that likely stimulate the ubiquitination process.

We examined the ubiquitination and UBA1 levels in oxRBCs from PrdxII$^{+/+}$ and PrdxII$^{-/-}$ mice. As shown in Fig. 1A, ubiquitination were sustained for 90 min in the membrane fraction of RBCs and oxRBCs from PrdxII$^{+/+}$ mice (top panel, lanes 1–5). During the same period, the UBA1 level time-dependently increased in membranes of oxRBCs (second panel, lanes 3 and 5) but not RBCs (second panel, lanes 2 and 4), and the overall ubiquitination level in the membrane fraction from PrdxII$^{-/-}$ RBCs was 3× higher than in PrdxII$^{+/+}$ RBCs (top panel, compare lanes 1–5 with lanes 6–10). Interestingly, ubiquitination was reduced by about 75% in PrdxII$^{-/-}$ oxRBCs after oxidation for 90 min (top panel, compare lanes 6–9 with lane 10), even though UBA1 levels were slightly increased (second panel, lane 10). In the cytosol fraction, both ubiquitination and the UBA1 levels were increased at 60 min and then decreased at 90 min in oxRBCs from both PrdxII$^{+/+}$ and PrdxII$^{-/-}$ (Fig. 1B, compare lanes 3 and 8 with lanes 5 and 10). However, there was no relationship between the ubiquitination and UBA1 levels. Although UBA1 levels increased over time in RBCs, ubiquitination remained constant (Fig. 1B, compare lanes 2 and 7 with lanes 4 and 9). These results suggest that the ubiquitination levels are determined by UBA1 activity, not the level of UBA1 protein.

3.2. Oxidative stress induces translocation of UBA1 to the plasma membrane

Fig. 1B shows that ubiquitination in the cytosol fraction declines over time to a greater degree in PrdxII$^{-/-}$ than PrdxII$^{+/+}$ oxRBCs (top panel, compare lanes 3 and 8 with lanes 5 and 10). The mechanism underlying the difference remains unclear, however. Based on the results summarized above, UBA1 activity is a critical determinant of the ubiquitination level, and there are numerous factors that can affect the enzyme's activity. Among those is its reduction/oxidation status, which is highly important because UBA1 possesses a catalytic cysteine.

To determine the redox status of UBA1, we examined PrdxII$^{+/+}$ and PrdxII$^{-/-}$ RBCs in which UBA1 was labeled with BIAM, which binds to free thiols (–SH) but not disulfide bonds (S–S) or hyperoxidized cysteines (–SOH, –SOOH). As shown in Fig. 2A, total UBA1

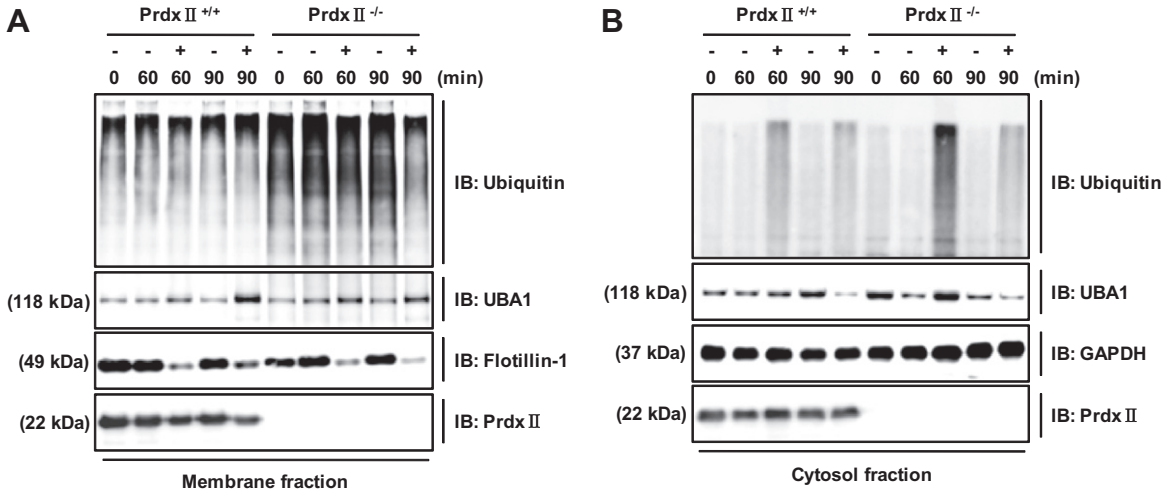

Fig. 1. Determination of the ubiquitination level based on UBA1 activity. (A) Membrane proteins (20 μg) were resolved by 10% SDS–PAGE, transferred to PVDF membranes, and immunoblotted with anti-ubiquitin, anti-UBA1, anti-flotillin-1 and anti-PrdxII antibodies. (B) Cytosolic proteins (40 μg) were separated by 10% SDS–PAGE and immunoblotted with anti-ubiquitin, anti-UBA1, anti-GAPDH and anti-PrdxII antibodies. Flotillin-1 and GAPDH were used as plasma membrane and cytosolic markers, respectively. –, Left untreated; +, treated with 0.2 mM $CuSO_4$ and 5 mM ascorbic acid.

levels did not differ between PrdxII$^{+/+}$ and PrdxII$^{-/-}$ RBCs (third panel). In addition, the level of BIAM labeling of UBA1 also did not differ between the cytosol fractions of PrdxII$^{+/+}$ and PrdxII$^{-/-}$ RBCs (second panel). By contrast, BIAM labeling of UBA1 in the membrane fraction from PrdxII$^{-/-}$ RBCs was a much greater degree in PrdxII$^{+/+}$ RBCs (first panel, compare lanes 1–3 with lanes 4–6). These results raise the question: how is the redox status of UBA1 changed under oxidative stress.

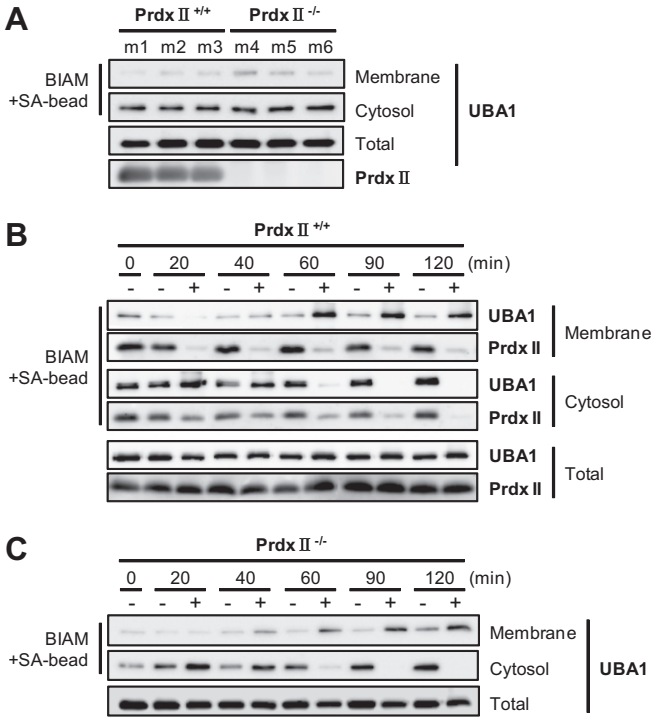

Fig. 2. Oxidative stress induces UBA1 membrane translocation. (A) Level of BIAM-labeled UBA1 in RBCs from PrdxII$^{+/+}$ (m1–m3) and PrdxII$^{-/-}$ (m4–m6) mice. (B) Representative gel image of BIAM-binding to UBA1 and PrdxII. Cysteine oxidation in UBA1 and PrdxII was confirmed in the membrane and cytosol fractions of oxRBCs. Total UBA1 and PrdxII levels were examined in PrdxII$^{+/+}$ RBCs. (C) Levels of total BIAM-labeled UBA1 in PrdxII$^{-/-}$ RBCs. Samples were run in triplicate. –, Left untreated; +, treated with 0.2 mM $CuSO_4$ and 5 mM ascorbic acid.

To address that question, we compared the levels of BIAM-labeled UBA1 in PrdxII$^{+/+}$ and PrdxII$^{-/-}$ oxRBCs. As shown in Fig. 2B, BIAM-labeled UBA1 in the cytosol fraction of PrdxII$^{+/+}$ oxRBCs remained unchanged during oxidation for up to 40 min and was then reduced at 60–120 min (second panel). Correspondingly, BIAM-labeled UBA1 levels in the membrane fraction were increased at 60–120 min (first panel). We observed a similar pattern in PrdxII$^{-/-}$ oxRBCs (Fig. 2C). Notably, total BIAM-labeled UBA1 in PrdxII$^{+/+}$ and PrdxII$^{-/-}$ oxRBCs was unchanged over the entire 120-min observation period (Fig. 2B and C). These results suggest that reduced UBA1 localizes mainly in the cytosol, but is translocated from the cytosol to the membrane under conditions of oxidative stress.

Neurodegenerative diseases such as Parkinson's disease (PD) and Alzheimer's disease (AD) are closely associated with the accumulation of protein aggregates such as amyloid beta (Aβ), alpha-synuclein, and tau. Interestingly, diminished proteasome activity is a key feature of cells that express aggregation-prone proteins [11]; however, its role, if there is any, in the pathogenesis of these diseases is unknown. It has been reported that UBA1 expression in the midbrain is reduced by 0.76-fold of a PD model mouse [12], and by 0.19-fold in RBCs from AD subjects, as compared to healthy controls [13]. Similar changes were observed in the cytosol fraction of the AD brain [14]. In addition, Lopez Salon et al. suggested that delocalization of UBA1 to the particulate fraction reduces its activity and impairs ubiquitination in the cytosol of the AD brain [14].

Cysteine residues in certain proteins are reportedly susceptible to oxidation in PrdxII$^{-/-}$ mice [6,7]. However, BIAM labeling of UBA1 in the membrane was greater in PrdxII$^{-/-}$ RBCs than in PrdxII$^{+/+}$ RBCs (Fig. 2A). The reduced forms of two cysteines were identified in the K2 fraction (Table S1). The ratio of reduced Cys-340 was W1>K1>K2, while reduced Cys-278 was found exclusively in the abnormal PrdxII$^{-/-}$ RBCs (K2 fraction). There was no apparent compensation for loss of PrdxII function in PrdxII$^{-/-}$ RBCs; that is, the activities and expression levels of other antioxidant enzymes such as GPx (glutathione peroxidase) and catalase were unchanged in PrdxII$^{-/-}$ RBCs [7]. It is therefore unclear what antioxidant is providing reducing power to UBA1.

Among known RBC abnormalities, the incidence of Heinz body formation is up to 30% higher in PrdxII$^{-/-}$ RBCs than either wild-type (PrdxII$^{+/+}$) RBCs or the heterozygotes [7]. From an oxidative stress point of view, the increased Heinz body formation may be

explained by following conditions. First, ubiquitination levels were lower in the cytosol of RBCs than in the membrane (Fig. 1). Second, the rate of decline in ubiquitination was greater in PrdxII$^{-/-}$ RBCs than in PrdxII$^{+/+}$ RBCs (Fig. 1). Finally, reduced UBA1, which localizes in the cytosol, was translocated to the membrane under oxidative stress (Fig. 2).

3.3. Decreased ubiquitination with the UBA1 C278S mutant

Mouse UBA1 contains 21 cysteine residues that are sensitive to oxidation (Fig. S1, Table S1), and although it is known that UBA1 activity is closely related to the oxidation state of its cysteine residues, it is unknown which cysteines are affected and impair ubiquitination under oxidative stress.

To identify the cysteines affecting ubiquitination, we designed five cysteine mutants and examined *in vivo* ubiquitination in the lysates of HEK293T and CMT93 cells expressing either UBA1 wild-type (WT) or a cysteine mutant. As shown in Fig. 3A, the levels of Ub adducts were decreased in cells expressing UBA1(C278S) or UBA1(C632S), as compared to UBA1(WT) or another cysteine mutant. With respect to UBA1(C632S), the cause of the decrease in Ub adduct is most likely the loss of the catalytic thiol. However, the catalytic cysteine is still intact in UBA1(C278S); nonetheless, ubiquitination was as low as with the C632S mutant. Two possible explanations are that the decrease in Ub adducts reflect the decreased stability of UBA1(C278S), or that there was a loss of Ub charging. To examine whether the stability of UBA1(WT) or the cysteine mutants is decreased by oxidative stress (H_2O_2 treatment), UBA1 expression was measured in HEK293T and CMT93 cells pretreated with cycloheximide. As shown in Fig. 3B, expression of UBA1(WT) and the cysteine mutants in HEK293T and CMT93 cells was unaffected by exposing the cells to H_2O_2 for up to 6 h, indicating that the decreased ubiquitination was not the result of a loss of stability. Instead, the decrease in ubiquitination was more likely due to a reduction in UBA1(C278S) activity toward the Ub substrate. These results also suggest that UBA1 Cys-278 may participate in Ub charging independently or in cooperation with Cys-632.

3.4. UBA1 Cys-278 participates in ubiquitin charging through a change in proximity

To determine the function of UBA1 Cys-278, *in vitro* ubiquitination assays were performed using recombinant UBA1 WT, C278S and C632S. As shown in Fig. 4A, all three proteins produced a slowly migrating band that conjugated with Ub (lower panel), and the resultant His-UBA1∼Ub conjugate was sensitive to a reducing agent (i.e., 2-mercaptoetanol) (upper panel). His-UBA1(WT)∼Ub levels declined rapidly, and the conjugate was nearly gone within 10 min (lower panel, lanes 1–4). By contrast, His-UBA1(C278S)∼Ub and His-UBA1(C632S)∼Ub conjugates persisted for 30 min (lower panel, lanes 5–9). One possible explanation for the loss of His-UBA1(WT)∼Ub is ATP depletion. In addition, His-UBA1(C632S)∼Ub may persist longer than His-UBA1(WT)∼Ub (lower panel, compare lanes 4 and 9) due to formation of an oxyester bond with Ub, which is a more stable bond than a thioester [15–18]. The catalytic cysteine in UBA1(C278S) remains intact, but migration of His-UBA1(C278S)∼Ub showed a pattern more similar to His-UBA1(C632S)∼Ub than to His-UBA1(WT)∼Ub (lower panel, compare lane 4 with lanes 8 and 9).

To further examine the activity of His-UBA1(C278S)∼Ub, a Ub transfer assay was performed using recombinant mouse E2A (RAD6 homolog; GenBank ID: BC026053), which belongs to the Ubc2 family. The amino acid sequence of mouse E2A is identical to its human ortholog (data not shown), and also has Ub charging activity [19]. As shown in Fig. 4B, His-UBA1∼Ub conjugates were generated with UBA1(WT), -(C278S) and -(C632S), and the levels of the C278S mutant conjugate were higher than the wild-type conjugate (first panel), which is consistent with the results summarized in Fig. 4A (lower panel). Ub transfer from UBA1 to E2A to form His-E2A∼Ub gradually reduced the levels of UBA1(WT) (second panel, lanes 1–4), but little His-E2A∼Ub conjugate was formed in the presence of UBA1(C278S) (second panel, lanes 5–8).

Using kinetic analyses, Siepmann et al. examined the binding affinity of HsUbc2b, HsUbc2bC88A and HsUbc2bC88S to human E1 [17]. The transthiolation kinetic constant for HsUbc2bC88S (1.7×10^{-3} s^{-1}) is considerably slower than for wild-type HsUbc2b

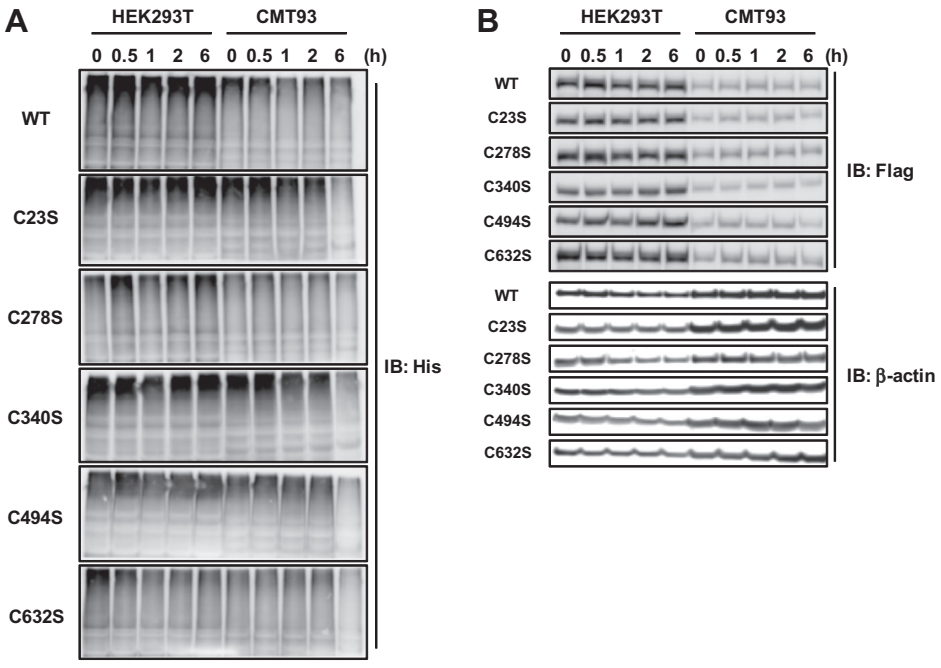

Fig. 3. Loss of ubiquitination reflects decreased UBA1 activity. (A) Cell lysates were harvested after exposure to H_2O_2 for the indicated times. Ub adducts were assessed by western blotting using anti-His antibody. (B) The membranes were then stripped and reprobed with anti-Flag antibody to measure exogenous UBA1 expression in wild-type (WT) UBA1 and the cysteine mutants. β-actin was used as a loading control.

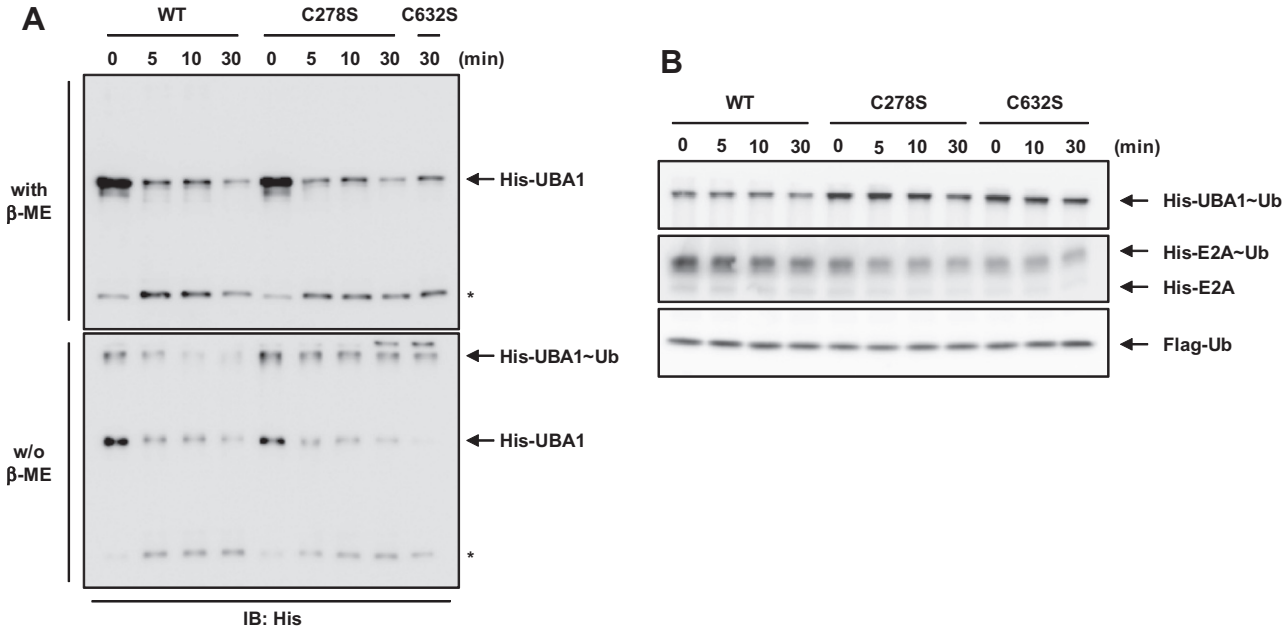

Fig. 4. Role of Cys-278 for Ub charging. (A) Reactants were divided equally and resolved on reducing or non-reducing 10% SDS–PAGE gels. UBA1∼Ub conjugates were analyzed by immunoblotting using anti-His antibody. Asterisks indicate non-specific bands. (B) The products were subjected to non-reducing 10% SDS–PAGE followed by immunoblotting with anti-His antibody.

($5\ s^{-1}$). In addition, the K_m value for the binding of HsUbc2bC88S (169 ± 17 nM) to E1 is higher than the value for HsUbc2b binding (119 ± 9 nM). Transthiolation is readily reversible when ATP is depleted or excess AMP and PPi are present [20], which diminishes the wild-type HsUbc2b adduct [17]. On the other hand, the HsUbc2bC88S∼Ub oxyester adduct was not reduced when AMP and PPi were added to the reaction mixture. It was concluded that the HsUbc2bC88S oxyester adduct is irreversible and catalytically inert.

Like Siepmann et al., we assumed that UBA1(WT) possesses greater affinity for E2A than UBA1(C632S). Consequently, the ubiquitin transfer process is faster with the wild-type proteins than with the C632S mutant, resulting in greater production of end products (His-E2A∼Ub) with the wild-type (Fig. 4B, second panel, compare lanes 1–4 with lanes 9–11).

As mentioned, UBA1(WT) readily proceeded from Ub charging to transthiolation, whereas UBA1(C632S) retained Ub within its catalytic pocket through stable oxyester bonding, which also retarded Ub transfer to the cognate E2A (Fig. 4B, second panel, compare lanes 1–4 with lanes 9–11).

In both *in vivo* and *in vitro* experiments, UBA1(C278S) behaved in a manner very similar to UBA1(C632S). This suggests that Cys-278 of UBA1 also participates in Ub charging, either independently of Cys-632 or in cooperation with it. However, no functional studies of UBA1 Cys-278 have yet been performed, in large part because the presence of four hyperoxidized cysteines is unique to mammals (human, mouse and rat) and is not conserved in wheat or yeast (Fig. S1).

At present, characterization of the structure of mammalian UBA1 is limited to the mouse. Furthermore, only the SCCH (PDB ID: 1Z7L) and FCCH (PDB ID: 2V31) domains of mouse UBA1 are available [21,22]. But since the crystal structure of UBA1 from yeast (*Saccharomyces cerevisiae*; PDB ID: 3CMM) has been solved [23], it is possible predict the catalytic mechanism of human E1. Yeast UBA1 and human UBE1 display over 50% amino acid sequence identity, and the structural domains are highly conserved.

Within the crystal structure of yeast UBA1, catalytic Cys-600 (Cys-632 in the mouse analog, Fig. S1) is 35 Å away from the Ub adenylation site [23]. That means a conformational change in the catalytic domain would be required to bring Ub into proximity with the catalytic cysteine. Brahemi et al. reported that UBA1∼Ub binding induces a significant shift of the C-terminal tail of Ub, as compared to the free protein [24]. This suggests that SCCH (i.e., the catalytic Cys domain) undergoes a conformational change when the thioester bond forms between the C-terminal of Ub and Cys-632 of UBA1.

The Gly-241 position within the structure of yeast UBA1 corresponds to Cys-278 in mouse UBA1. Gly-241 is exposed to the exterior in the FCCH domain and is easily accessible to the solvent, although it is still >40 Å away from the C-terminal of Ub. However, the SCCH and FCCH domains are linked by extended loops suggesting movement of the tail could induce a conformational change in SCCH and FCCH. We therefore suggest that Cys-278 can be involved in Ub charging if FCCH undergoes a conformational change similar to the motion of the catalytic Cys domain.

Taken together, these results suggest that Cys-278 participates in Ub charging through a change in its proximity to Ub, most likely contributing to an alteration in structural conformation, not a directly interaction at the UBA1–Ub interface.

In summary, ubiquitination levels are strongly related to UBA1 activity. Our results suggest that impaired ubiquitination in the cytosol is caused by translocation of UBA1 to the membrane under oxidative stress. UBA1 Cys-278 is sensitive to oxidation and can affect Ub charging through a change in its proximity to Ub.

Acknowledgments

This study was supported by the National Research Foundation of Korea (NRF) grant funded by the Korea government (MEST) (No. 2012-0000415), and by a grant of the Korean Health Technology R&D Project, Ministry of Health & Welfare (A111455), Republic of Korea.

Appendix A. Supplementary data

Supplementary data associated with this article can be found, in the online version, at http://dx.doi.org/10.1016/j.bbrc.2012.09.102.

References

[1] A. Hershko, A. Ciechanover, A. Varshavsky, Basic Medical Research Award. The ubiquitin system, Nat. Med. 6 (2000) 1073–1081.

[2] A. Hershko, A. Ciechanover, The ubiquitin system for protein degradation, Annu. Rev. Biochem. 61 (1992) 761–807.

[3] L. Gong, E.T. Yeh, Identification of the activating and conjugating enzymes of the NEDD8 conjugation pathway, J. Biol. Chem. 274 (1999) 12036–12042.

[4] P.M. Hatfield, R.D. Vierstra, Multiple forms of ubiquitin-activating enzyme E1 from wheat. Identification of an essential cysteine by *in vitro* mutagenesis, J. Biol. Chem. 267 (1992) 14799–14803.

[5] M.T. Forrester, D.T. Hess, J.W. Thompson, R. Hultman, M.A. Moseley, J.S. Stamler, P.J. Casey, Site-specific analysis of protein S-acylation by resin-assisted capture, J. Lipid Res. 52 (2011) 393–398.

[6] H.Y. Yang, J. Kwon, H.I. Choi, S.H. Park, U. Yang, H.R. Park, L. Ren, K.J. Chung, Y.U. Kim, B.J. Park, S.H. Jeong, T.H. Lee, In-depth analysis of cysteine oxidation by the RBC proteome: advantage of peroxiredoxin II knockout mice, Proteomics 12 (2012) 101–112.

[7] T.H. Lee, S.U. Kim, S.L. Yu, S.H. Kim, D.S. Park, H.B. Moon, S.H. Dho, K.S. Kwon, H.J. Kwon, Y.H. Han, S. Jeong, S.W. Kang, H.S. Shin, K.K. Lee, S.G. Rhee, D.Y. Yu, Peroxiredoxin II is essential for sustaining life span of erythrocytes in mice, Blood 101 (2003) 5033–5038.

[8] G.R. Sambrano, S. Parthasarathy, D. Steinberg, Recognition of oxidatively damaged erythrocytes by a macrophage receptor with specificity for oxidized low density lipoprotein, Proc. Natl. Acad. Sci. USA 91 (1994) 3265–3269.

[9] V. Terpstra, T.J. van Berkel, Scavenger receptors on liver Kupffer cells mediate the in vivo uptake of oxidatively damaged red blood cells in mice, Blood 95 (2000) 2157–2163.

[10] G.R. Sambrano, V. Terpstra, D. Steinberg, Independent mechanisms for macrophage binding macrophage phagocytosis of damaged erythrocytes evidence of receptor cooperativity, Arterioscler. Thromb. Vasc. Biol. 17 (1997) 3442–3448.

[11] N.F. Bence, R.M. Sampat, R.R. Kopito, Impairment of the ubiquitin–proteasome system by protein aggregation, Science 292 (2001) 1552–1555.

[12] M. Diedrich, T. Kitada, G. Nebrich, A. Koppelstaetter, J. Shen, C. Zabel, J. Klose, L. Mao, Brain region specific mitophagy capacity could contribute to selective neuronal vulnerability in Parkinson's disease, Proteome Sci. 9 (2011) 59.

[13] J.G. Mohanty, H.D. Shukla, J.D. Williamson, L.J. Launer, S. Saxena, J.M. Rifkind, Alterations in the red blood cell membrane proteome in Alzheimer's subjects reflect disease-related changes and provide insight into altered cell morphology, Proteome Sci. 8 (2010) 11.

[14] M. Lopez Salon, L. Morelli, E.M. Castano, E.F. Soto, J.M. Pasquini, Defective ubiquitination of cerebral proteins in Alzheimer's disease, J. Neurosci. Res. 62 (2000) 302–310.

[15] M. Komatsu, T. Chiba, K. Tatsumi, S. Iemura, I. Tanida, N. Okazaki, T. Ueno, E. Kominami, T. Natsume, K. Tanaka, A novel protein-conjugating system for Ufm1 a ubiquitin-fold modifier, EMBO J. 23 (2004) 1977–1986.

[16] J.N. Pruneda, K.E. Stoll, L.J. Bolton, P.S. Brzovic, R.E. Klevit, Ubiquitin in motion: structural studies of the ubiquitin-conjugating enzyme approximately ubiquitin conjugate, Biochemistry 50 (2011) 1624–1633.

[17] T.J. Siepmann, R.N. Bohnsack, Z. Tokgoz, O.V. Baboshina, A.L. Haas, Protein interactions within the N-end rule ubiquitin ligation pathway, J. Biol. Chem. 278 (2003) 9448–9457.

[18] R. Hjerpe, Y. Thomas, J. Chen, A. Zemla, S. Curran, N. Shpiro, L.R. Dick, T. Kurz, Changes in the ratio of free NEDD8 to ubiquitin triggers NEDDylation by ubiquitin enzymes, Biochem. J. 441 (2012) 927–936.

[19] J. Jin, X. Li, S.P. Gygi, J.W. Harper, Dual E1 activation systems for ubiquitin differentially regulate E2 enzyme charging, Nature 447 (2007) 1135–1138.

[20] A.L. Haas, P.M. Bright, The resolution and characterization of putative ubiquitin carrier protein isozymes from rabbit reticulocytes, J. Biol. Chem. 263 (1988) 13258–13267.

[21] R.H. Szczepanowski, R. Filipek, M. Bochtler, Crystal structure of a fragment of mouse ubiquitin-activating enzyme, J. Biol. Chem. 280 (2005) 22006–22011.

[22] L. Jaremko, M. Jaremko, R. Filipek, M. Wojciechowski, R.H. Szczepanowski, M. Bochtler, I. Zhukov, NMR assignment of a structurally uncharacterised fragment of recombinant mouse ubiquitin-activating enzyme, J. Biomol. NMR 36 (Suppl. 1) (2006) 43.

[23] I. Lee, H. Schindelin, Structural insights into E1-catalyzed ubiquitin activation and transfer to conjugating enzymes, Cell 134 (2008) 268–278.

[24] G. Brahemi, A.M. Burger, A.D. Westwell, A. Brancale, Homology modelling of human E1 ubiquitin activating enzyme, Lett. Drug Des. Discov. 7 (2010) 57–62.